JPP Journal of Pharmacy and Pharmacology

JPP 2008, 60: 1365–1374

Received February 27, 2008
Accepted June 5, 2008
DOI 10.1211/jpp/60.10.0013
ISSN 0022-3573

Astaxanthin, a dietary carotenoid, protects retinal cells against oxidative stress in-vitro and in mice in-vivo

Yoshimi Nakajima, Yuta Inokuchi, Masamitsu Shimazawa, Kazumasa Otsubo, Takashi Ishibashi and Hideaki Hara

Abstract

We have investigated whether astaxanthin exerted neuroprotective effects in retinal ganglion cells in-vitro and in-vivo. In-vitro, retinal damage was induced by 24-h hydrogen peroxide (H_2O_2) exposure or serum deprivation, and cell viability was measured using a WST assay. In cultured retinal ganglion cells (RGC-5, a rat ganglion cell-line transformed using E1A virus), astaxanthin inhibited the neurotoxicity induced by H_2O_2 or serum deprivation, and reduced the intracellular oxidation induced by various reactive oxygen species (ROS). Furthermore, astaxanthin decreased the radical generation induced by serum deprivation in RGC-5. In mice in-vivo, astaxanthin (100 mg kg^{-1}, p.o., four times) reduced the retinal damage (a decrease in retinal ganglion cells and in thickness of inner plexiform layer) induced by intravitreal *N*-methyl-D-aspartate (NMDA) injection. Furthermore, astaxanthin reduced the expressions of 4-hydroxy-2-nonenal (4-HNE)-modified protein (indicator of lipid peroxidation) and 8-hydroxy-deoxyguanosine (8-OHdG; indicator of oxidative DNA damage). These findings indicated that astaxanthin had neuroprotective effects against retinal damage in-vitro and in-vivo, and that its protective effects may have been partly mediated via its antioxidant effects.

Department of Biofunctional Evaluation, Molecular Pharmacology, Gifu Pharmaceutical University, 5-6-1 Mitahora-higashi, Gifu 502-8585, Japan

Yoshimi Nakajima, Yuta Inokuchi, Masamitsu Shimazawa, Hideaki Hara

Fine Chemicals Marketing Department, Fine Chemicals Division, Asahi Kasei Pharma Corporation, 9-1 Kanda Mitoshiro-cho, Chiyoda-ku, Tokyo 101-8481, Japan

Kazumasa Otsubo

Biotechnology Business Section, Merchandise Business Department, Nippon Oil Corporation, 3-12 Nishi Shimbashi 1-chome, Minato-ku, Tokyo 105-8412, Japan

Takashi Ishibashi

Correspondence: H. Hara, Department of Biofunctional Evaluation, Molecular Pharmacology Gifu Pharmaceutical University, 5-6-1 Mitahora-higashi, Gifu 502-8585, Japan.
E-mail: hidehara@gifu-pu.ac.jp

Introduction

Astaxanthin, a dietary carotenoid, is present in many biological systems, often decreasing the formation of products of oxidative damage induced by biological molecules. Astaxanthin is a powerful biological antioxidant occurring naturally in a wide variety of living organisms (Clarke et al 1990), and is present in many well-known sea foods such as salmon, trout, red sea-bream, shrimp, lobster and fish eggs. Astaxanthin possesses various pharmacological activities, including antioxidative activity (Kurashige et al 1990; O'Connor & O'Brien 1998; Iwamoto et al 2000; Kobayashi 2000; Aoi et al 2003), antitumour effects (Chew et al 1999a; Jyonouchi et al 2000), an anti-inflammatory action (Ohgami et al 2003), antidiabetic (Uchiyama et al 2002) and hepatoprotective effects (Kang et al 2001), and immunomodulatory activity (Okai & Higashi-Okai 1996; Chew et al 1999b). Thus, astaxanthin has considerable potential for applications in human health and nutrition.

Retinal ganglion cell (RGC) death is a common feature of many ophthalmic disorders, such as glaucoma, optic neuropathies, and various retinovascular diseases (diabetic retinopathy and retinal vein occlusions) (Bocker-Meffert et al 2002). RGC death may occur via a variety of mechanisms involving, for example, reactive oxygen species (ROS) (Bonne et al 1998), excitatory amino acids (Dreyer 1998), nitric oxide (Neufeld 1999) and apoptosis (McKinnon 1997). Previous studies on the protective effects of carotenoids (including astaxanthin) against retinal damage have primarily focused on age-related maculopathy (Parisi et al 2008). Moreover, to our knowledge no examination has been made of the in-vitro neuroprotective effects of astaxanthin against oxidative stress using retinal ganglion cells or in-vivo models of retinal damage.

The purpose of this study was to examine the effects of astaxanthin on retinal damage in-vitro and in-vivo. We studied its effects on hydrogen peroxide (H_2O_2)-induced or serum deprivation-induced neurotoxicity in RGC-5 (a rat ganglion cell-line transformed using E1A virus) cultures, on the intracellular oxidation induced by various ROS in RGC-5 cultures, and on in-vivo *N*-methyl-D-aspartate (NMDA)-induced retinal damage in mice.

In addition, we examined its effects on the accumulation of lipid peroxidation and oxidative DNA damage observed at 12 h after NMDA intravitreal injection in mice.

Materials and Methods

Materials

RGC-5 was a gift from Dr Neeraj Agarwal (UNT Health Science Center, Fort Worth, TX, USA). Drugs and sources were as follows: Dulbecco's modified Eagle's medium (DMEM), trolox (a derivative of α-tocopherol, water-soluble vitamin E) and NMDA were purchased from Sigma-Aldrich (St Louis, MO, USA). Fetal bovine serum (FBS) was from Valeant (Costa Mesa, CA, USA). Dimethyl sulfoxide (DMSO) and olive oil were from Nacarai Tesque Inc. (Kyoto, Japan). Penicillin and streptomycin were from Meiji Seika Kaisha Ltd (Tokyo, Japan). Isoflurane was from Nissan Kagaku (Tokyo, Japan). Cell Counting Kit-8 was from Dojin Kagaku (Kumamoto, Japan). H_2O_2 and iron (II) perchlorate hexahydrate were from Wako (Osaka, Japan). KO_2 was from Aldrich Chemical Company, Inc. (Milwaukee, WI, USA). Hoechst 33342 and 5-(and-6)-chloromethyl-2′,7′-dichlorodihydrofluorescein diacetate acetyl ester (CM-H_2DCFDA) were from Molecular Probes (Eugene, OR, USA). Astaxanthin was the free form derived from *Paracoccus carotinifaciens* (Asahi Kasei Pharma. Co., Tokyo, Japan). The purity of astaxanthin and carotenoid was 60 and 99%, respectively.

Retinal ganglion cell line (RGC-5) culture

RGC-5 cells were maintained in DMEM containing 10% FBS, 100 U mL^{-1} penicillin and 100 μg mL^{-1} streptomycin under a humidified atmosphere of 95% air and 5% CO_2 at 37°C. The RGC-5 cells were passaged by trypsinization every three to four days, as described by Shimazawa et al (2005).

To examine the effects of astaxanthin at 0.01–10 nM or trolox at 10–100 μM on the cell death induced by 0.3 mM H_2O_2, RGC-5 cells were seeded at a low density of 1×10^3 cells/well into 96-well plates. After pretreatment with astaxanthin or trolox for 1 h, H_2O_2 was added to these cultures for 24 h.

To examine the effects of astaxanthin at 10 nM or trolox at 100 μM on the cell death induced by serum deprivation, RGC-5 cells were seeded at a low density of 1×10^3 cells/well into 96-well plates. After incubating for one day, cells were exposed to serum-free medium plus astaxanthin, trolox, or vehicle (1% DMSO phosphate-buffered saline; PBS) for 24 h.

Cell viability

To evaluate cell survival, we examined the change in fluorescence intensity following the cellular reduction of WST-8 to formazan. All experiments were performed in DMEM at 37°C. Cell viability was assessed by culturing cells in a culture medium containing 10% WST-8 (Cell Counting Kit-8) for 3 h at 37°C, then examining the absorbance at 492 nm. This fluorescence was expressed as a percentage of that in control cells (which were in 1% FBS DMEM), after subtraction of background fluorescence.

Hoechst 33342 staining

At the end of the culture period, Hoechst 33342 (excitation at 360 nm, emission at 490 nm) was added to the culture medium for 15 min at a final concentration of 8.1 μM. Images were collected using a CCD camera (DP30BW; Olympus. Co., Tokyo, Japan). Hoechst 33342-positive cells were taken as the total number of cells present, since Hoechst 33342 stains live and dead cells.

Reactive oxygen species detection

To evaluate the cellular radicals induced by serum deprivation, cells were examined under the fluorescence microscope. Experiments were performed in DMEM at 37°C. Cells were exposed to serum-free medium with or without astaxanthin for 6 h. A cellular radical probe, CM-H_2DCFDA, and Hoechst 33342 were then added in serum-free DMEM for 20 min. Moreover, an inhibitor of anion transport, probenecid, was added to these cultures. Images were collected using a CCD camera (Olympus Co., Tokyo, Japan). Radical intensity was measured using Metamorph (Meta imaging Series 6.1, Molecular Devices, Sunnyvale, CA, USA).

Radical scavenging-capacity assay

Radical species (H_2O_2, $O_2{\cdot}^-$, HO·) oxidize nonfluorescent dichlorofluorescein (DCFH) to fluorescent dichlorofluorescein (DCF). Experiments were performed in DMEM medium at 37°C. Cells were washed in 1% FBS DMEM with or without astaxanthin for 1 h. The cellular radical probe CM-H_2DCFDA was added for 20 min and cells were washed with 1% FBS DMEM with or without astaxanthin.

Fluorescence was measured after adding ROS-generating compounds for various time periods using excitation/emission wavelengths of 485/535 nm (Skanlt RE for Varioskan Flash 2.4; Thermo Fisher Scientific, Waltham, MA, USA). 'Radical integral' was calculated by integrating the area under the CM-H_2DCFDA fluorescence intensity curve for 20 min after ROS-generating compounds treatment. Results represented the averages ± s.e. of four independent experiments, with each treatment performed in duplicate.

Animals

Male adult ddY mice (36–43 g; Japan SLC, Hamamatsu, Japan) were kept under 12-h light/12-h dark conditions. All experimental procedures were approved and monitored by the Institutional Animal Care and Use Committee of Gifu Pharmaceutical University.

NMDA-induced retinal damage

Retinal damage was induced by NMDA as described by Siliprandi et al (1992). Briefly, anaesthesia was induced with 3.0% isoflurane and maintained with 1.5% isoflurane in

70% N_2O and 30% O_2 via an animal general anaesthesia machine (Soft Lander; Sin-ei Industry Co., Ltd, Saitama, Japan). Body temperature was maintained at between 37.0 and 37.5°C with the aid of a heating pad and heating lamp. Retinal damage was induced by the injection (2 μL/eye) of NMDA dissolved at 20 mM in 0.01 M PBS. This was injected into the vitreous body of the left eye under the above anaesthesia. One drop of 0.01% levofloxacin ophthalmic solution (Santen Pharmaceuticals Co. Ltd, Osaka, Japan) was applied topically to the treated eye immediately after the intravitreal injection. Seven days after the NMDA injection, eyeballs were enucleated for histological analysis.

Astaxanthin (100 mg kg^{-1}) was dissolved in olive oil immediately before use, and was orally administered four times (at 6 h before, and at 0, 6, and 24 h after the NMDA injection) for histological analysis, or three times (at 6 h before, and at 0 and 6 h after the NMDA injection) for TUNEL staining and immunostaining analysis with a volume of 0.1 mL/10 g body weight.

Histological analysis of mouse retina

Mice were anaesthetized by an intraperitoneal injection of sodium pentobarbital (80 mg kg^{-1}). Each eye was enucleated and kept immersed for at least 24 h at 4°C in a fixative solution containing 4% paraformaldehyde. Six paraffin-embedded sections (thickness, 4 μm) cut through the optic disc of each eye were prepared in a standard manner, and stained with haematoxylin and eosin. Retinal damage was evaluated as described by Yoneda et al (2001), three sections from each eye being used for the morphometric analysis. Light-microscope images were photographed, and the cell count in the ganglion cell layer (GCL) at a distance between 375 and 625 μm from the optic disc, and the thickness of the inner plexiform layer (IPL) were measured on the photographs in a masked fashion by a single observer (Y. Nakajima). Data from three sections (selected randomly from the six sections) were averaged for each eye, and these were used to evaluate the GCL cell count and IPL thickness.

TUNEL staining

TUNEL staining was performed according to the manufacturer's protocol (In Situ Cell Death Detection Kit; Roche Biochemicals, Mannheim, Germany) to detect the retinal cell death induced by NMDA. The mice (n = 8) were anaesthetized with pentobarbital sodium (80 mg kg^{-1}, i.p.) at 24 h after intravitreal injection of NMDA at 5 nmol/eye. The eyes were enucleated, fixed overnight in 4% paraformaldehyde solution in 0.1 M phosphate buffer (pH 7.4), and immersed for two days in PBS containing 25% sucrose. The eyes were then embedded in a supporting medium for frozen-tissue specimens (OCT compound; Tissue-Tek, Tokyo, Japan). Retinal sections 10-μm thick were cut on a cryostat at −25°C, and stored at −80°C until staining. After twice washing with PBS, sections were incubated with terminal deoxyribonucleotidyl transferase (TdT) enzyme at 37°C for 1 h. The sections were washed three times in PBS for 1 min at room temperature. Sections were subsequently incubated with an anti-fluorescein antibody–peroxidase (POD) conjugate at room temperature in a humidified chamber for 30 min, and then developed using diaminobenzidine(DAB) tetrahydrochloride peroxidase substrate. Light-microscope images were photographed (COOLPIX4500; Nikon, Tokyo), and the labelled cells were counted in the GCL at a distance between 375 and 625 μm from the optic disc in two central areas of the retina. The numbers of TUNEL-positive cells were averaged for the two areas, and this value was plotted as the number of TUNEL-positive cells.

Immunostaining

To detect 4-HNE (4-hydroxy-2-nonenal) and 8-OHdG (8-hydroxy-2′-deoxyguanosine) protein in the retina, immunostaining was performed. For this, the following primary antibodies were used: anti-4-HNE monoclonal antibody (clone HNEJ-2) and anti-8-OHdG monoclonal antibody (clone N45.1) (JaICA, Shizuoka, Japan). A total of 24 animals were used, and each eye was enucleated as described in 'Histological analysis', and then post-fixed overnight in 4% paraformaldehyde solution in 0.1 M phosphate buffer (pH 7.4) at 4°C, and embedded in paraffin. Cross sections (4 μm) through the optic nerve were obtained from the paraffin-embedded eyes. Such sections were deparaffinized with xylene and dehydrated through a graded ethanol series. Immunohistochemical staining was performed in accordance with the following protocol. Briefly, tissue sections were washed in 0.01 M PBS for 10 min, and then endogenous peroxidase was quenched by treating the sections with 3% hydrogen peroxide in absolute methanol for 10 min, followed by pre-incubation with VECTOR M.O.M. Immunodetection Kit (Vector Laboratories, Burlingame, CA, USA). A mouse monoclonal antibody against 4-HNE or 8-OHdG was added at a dilution of 1:1000. Sections were then incubated with primary antibodies overnight at 4°C. The slides were washed and incubated with biotinylated anti-mouse IgG. They were subsequently incubated with avidin–biotin–peroxidase complex for 30 min and developed using DAB peroxidase substrate. Light-microscope images were photographed, and the labelled cells were counted in the GCL at a distance between 375 and 625 μm from the optic disc in two central areas of the retina. The number of 8-OHdG-positive cells was averaged for the two areas, and this value was plotted as the number of 8-OHdG-positive cells. Light-microscope images were photographed (COOLPIX 4500; Nikon, Tokyo), and the DAB-labelled cells in the GCL and IPL at a distance between 475 and 525 μm (50×50 μm) from the optic disc were counted in two central areas of the retina. The retinal DAB-labelled density was evaluated by means of an appropriately calibrated computerized image analysis (Image J).

Statistical analysis

Data were presented as means ± s.e.m. Statistical significance, as indicated ($^*P < 0.05$, $^{**}P < 0.01$), was determined by one-way analysis of variance followed by a post-hoc

Dunnett and Tukey test, either of which compared with the vehicle as indicated in the figure.

Results

Effects of astaxanthin on cell damage induced by H_2O_2 in RGC-5 culture

Typical photographs of Hoechst 33342 staining are shown in Figure 1A–C. Non-treated control cells displayed normal nuclear morphology (Figure 1A). Cells treated with H_2O_2 for 24 h revealed shrinkage and condensation of their nuclei (Figure 1B). Astaxanthin (10 nM) decreased the nuclear condensation induced by H_2O_2 (Figure 1C). From our evaluation of cell viability (using Cell Counting Kit-8), 0.3 mM H_2O_2 treatment for 24 h reduced cell viability to approximately 40% of control. Astaxanthin at 0.1–10 nM significantly inhibited this decrease (Figure 1D), and the potency of astaxanthin was much the same as that of trolox (10 μM).

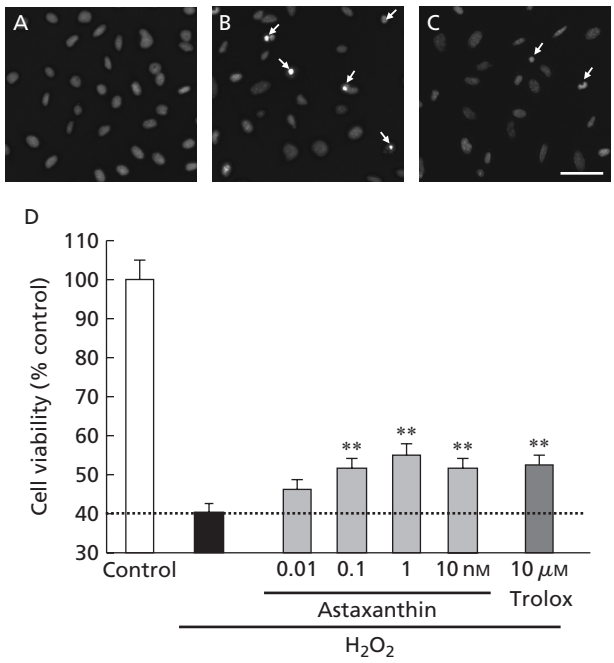

Figure 1 Effects of astaxanthin on cell damage induced by H_2O_2 in RGC-5 culture. (A–C) Representative fluorescence microscopy of Hoechst 33342 staining at 24 h after addition of H_2O_2. A. Non-treated cells showed normal nuclear morphology. B. H_2O_2 (0.3 mM)-induced neurotoxicity, with cells showing nuclear condensation (arrows). C. Pretreatment with 10 nM astaxanthin at 1 h before H_2O_2-treatment reduced nuclear condensation (arrows). D. Cell viability was assessed by immersing cells in WST-8 solution for 3 h at 37°C, with fluorescence being recorded at 492/660 nm. H_2O_2 induced a decrease in cell viability. Astaxanthin (0.1–10 nM) and trolox (10 μM) each significantly inhibited the H_2O_2-induced cell damage. Each column represents the mean ± s.e.m., n = 6. $^{**}P < 0.01$ v. H_2O_2-treatment alone. Scale bar = 50 μm.

Effects of astaxanthin on cell damage induced by serum deprivation in RGC-5 culture

Astaxanthin at a concentration of 10 nM inhibited serum deprivation-induced cell death in RGC-5 cell culture (Figure 2). Trolox (100 μM) also inhibited this cell death. To investigate the neuroprotective effects of astaxanthin against serum deprivation-induced oxidative stress, we determined the level of ROS in RGC-5 cells using a ROS-sensitive probe, CM-H_2DCFDA. Non-treated control cells supplemented with 1% FBS displayed little fluorescence intensity in the total cells (Figure 3A). Total cell number was on average 300–400 per one sight using Metamorph. Serum deprivation resulted in an increase in ROS production, as shown by increased DCF fluorescence (Figure 3B). Treatment with astaxanthin at 10 nM reduced the serum deprivation-induced ROS production (Figure 3C). For the evaluation of ROS production per cell, cellular radical intensity was quantified. Serum deprivation resulted in an 8-fold increase in ROS production (vs control), and astaxanthin (10 nM) reduced this ROS production to a similar extent as trolox (100 μM) (Figure 3D).

Effects of astaxanthin on the intracellular oxidation of DCFH induced by various types of ROS

To investigate the effect of astaxanthin on hydrogen peroxide (H_2O_2), superoxide anion ($O_2\cdot^-$), and hydroxyl radical (HO·) production, we employed a radical scavenging-capacity assay using a ROS-sensitive probe, CM-H_2DCFDA.

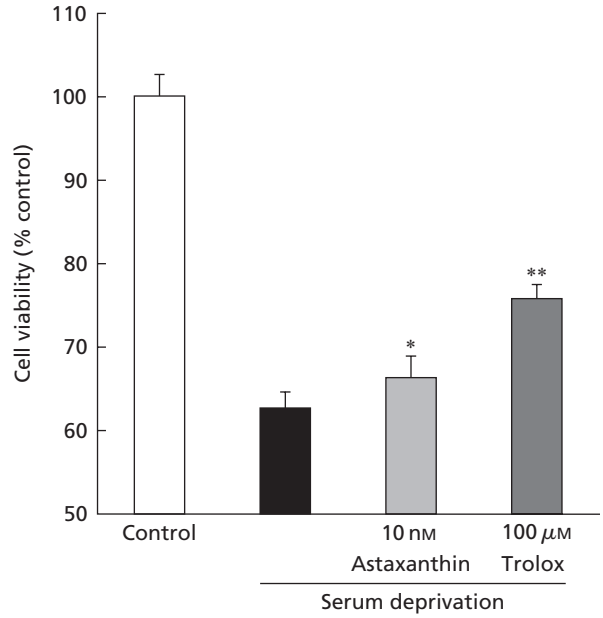

Figure 2 Effects of astaxanthin on cell damage induced by serum deprivation in RGC-5. Treatment with astaxanthin (10 nM) or trolox (100 μM) significantly reduced the retinal cell damage induced by serum deprivation. Cell viability was assessed by immersing cells in WST-8 solution for 3 h at 37°C, with fluorescence being recorded at 492/660 nm. Each column represents the mean ± s.e.m., n = 6. $^{*}P < 0.05$, $^{**}P < 0.01$ vs serum deprivation alone.

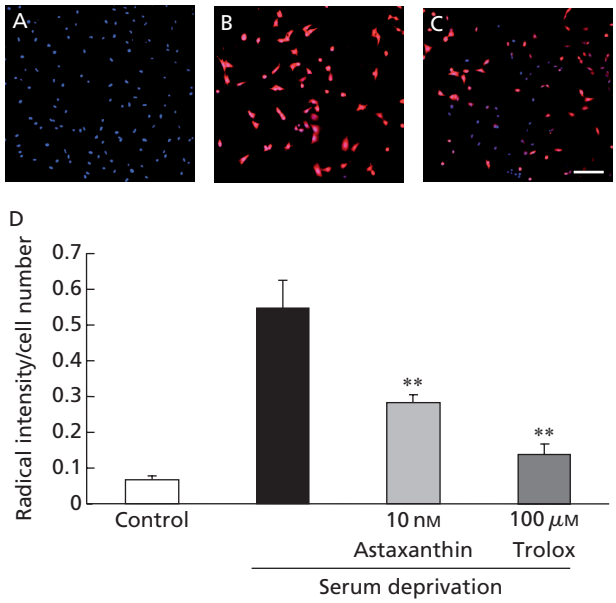

Figure 3 Scavenging effects of astaxanthin on serum deprivation-induced cellular radicals in RGC-5. (A–C) Representative fluorescence microscopy of Hoechst 33342 and radical-intensity staining at 6 h after serum deprivation. Light grey staining (as in A) is total cells at Hoechst 33342-positive cells. Dark grey staining (as in B) is CM-H_2DCFDA-positive cells to detect the radical production. Radical intensity was calculated as described in 'Methods'. A. Non-treated cells generated few radicals. B. Serum deprivation-induced neurotoxicity, with widespread generation of radicals. C. Treatment with astaxanthin (10 nM) markedly inhibited serum deprivation-induced generation of radicals. D. Cellular radical intensity was quantified by fluorescence microscopy of embedded probe, CM-H_2DCFDA. Serum deprivation induced ROS production, which was partly inhibited by astaxanthin (10 nM) and by trolox (100 μM). Each column represents the mean ± s.e.m., n = 6. $^{**}P < 0.01$ vs serum deprivation alone. Scale bar = 50 μm.

The kinetics of DCFH oxidation by ROS (monitored as fluorescence generation) are shown in Figure 4A–C. H_2O_2 radicals were generated by treatment with H_2O_2 at 100 μM, and astaxanthin at 10 or 100 nM significantly scavenged these H_2O_2 radicals (Figure 4D). $O_2\cdot^-$ was generated following treatment with KO_2 at 1 mM, and astaxanthin at 100 nM scavenged these $O_2\cdot^-$ radicals (Figure 4E). The HO· radicals generated by treatment with H_2O_2 at 1 mM plus Fe perchlorate (II) at 100 μM were scavenged by astaxanthin at 10 and 100 nM (Figure 4F).

Effects of astaxanthin on retinal damage induced by intravitreal injection of NMDA in mice

Intravitreal injection of NMDA at 5 nmol per eye decreased both the cell count in the GCL and the thickness of the IPL in the mouse retina (Figure 5B–E), as compared with those in the non-treated normal retina (Figure 5A). Treatment with astaxanthin (100 mg kg^{-1}, p.o., at 6 h before, and at 0, 6 and 24 h after the NMDA injection) significantly suppressed both of these decreases (Figure 5C–E).

Anti-apoptotic effects of astaxanthin against retinal damage

TUNEL-positive cells were observed in GCL and the upper layer of INL at 24 h after NMDA injection, as shown in Figure 6B (arrows), but none were seen in the untreated retina (Figure 6A). In the GCL of the astaxanthin-treated retina (Figure 6C), expression of TUNEL-positive cells was significantly reduced (vs the vehicle-treated retina) (Figure 6D).

Effects of astaxanthin on retinal oxidative DNA damage in mice

We identified oxidative DNA damage by means of an anti-8-OHdG antibody. No positive staining was detected in the normal (non-operated) eye (Figure 7A). At 12 h after NMDA injection, 8-OHdG immunoreactivity was evident in the nuclei of GCL (Figure 7B). Treatment with astaxanthin (100 mg kg^{-1}, p.o., at 6 h before, and at 0 and 6 h after the NMDA injection) significantly suppressed the increase in 8-OHdG positive cells in GCL (Figure 7C, D).

Effects of astaxanthin on retinal lipid peroxidation damage in mice

Lipid peroxidation was assessed using an anti-4-HNE antibody. In the normal (non-operated) eye, 4-HNE immunoreactivity was rarely observed (Figure 7E). At 12 h after NMDA injection, 4-HNE immunoreactivity was widespread in the GCL and IPL (Figure 7F). Treatment with astaxanthin (100 mg kg^{-1}, p.o., at 6 h before, and at 0 and 6 h after the NMDA injection) significantly suppressed the intensity of the immunoreactivity in 4-HNE-positive cells (vs the NMDA-treated, vehicle-treated control) (Figure 7G, H).

Discussion

In this study, we examined the in-vitro neuroprotective effects of astaxanthin against H_2O_2-induced and serum deprivation-induced cell damage, the production of cellular ROS following serum deprivation-stress, and ROS-induced intracellular oxidation in RGC-5 (an established transformed rat retinal ganglion cell-line) cultures. We also examined its effects against NMDA-induced retinal damage in mice in-vivo. The results indicated that astaxanthin exerted neuroprotective effects against in-vitro and in-vivo retinal damage, presumably by scavenging hydrogen peroxide (H_2O_2), superoxide anion ($O_2\cdot^-$), and hydroxyl radical (HO·).

Following treatment with H_2O_2 solution, the H_2O_2 radical is generated, and this induces superoxide ($O_2\cdot^-$) generation in mitochondria together with the Fenton reaction, in which a reduced transition metal, such as intracellular Fe^{2+} or Cu^{2+}, reduces H_2O_2 to form HO· and hydroxyl anion (Schlieve et al 2006). Furthermore, the predominant serum deprivation-induced ROS has been reported to be H_2O_2 (Kim et al 2000). The in-vitro neuroprotective effect of astaxanthin against

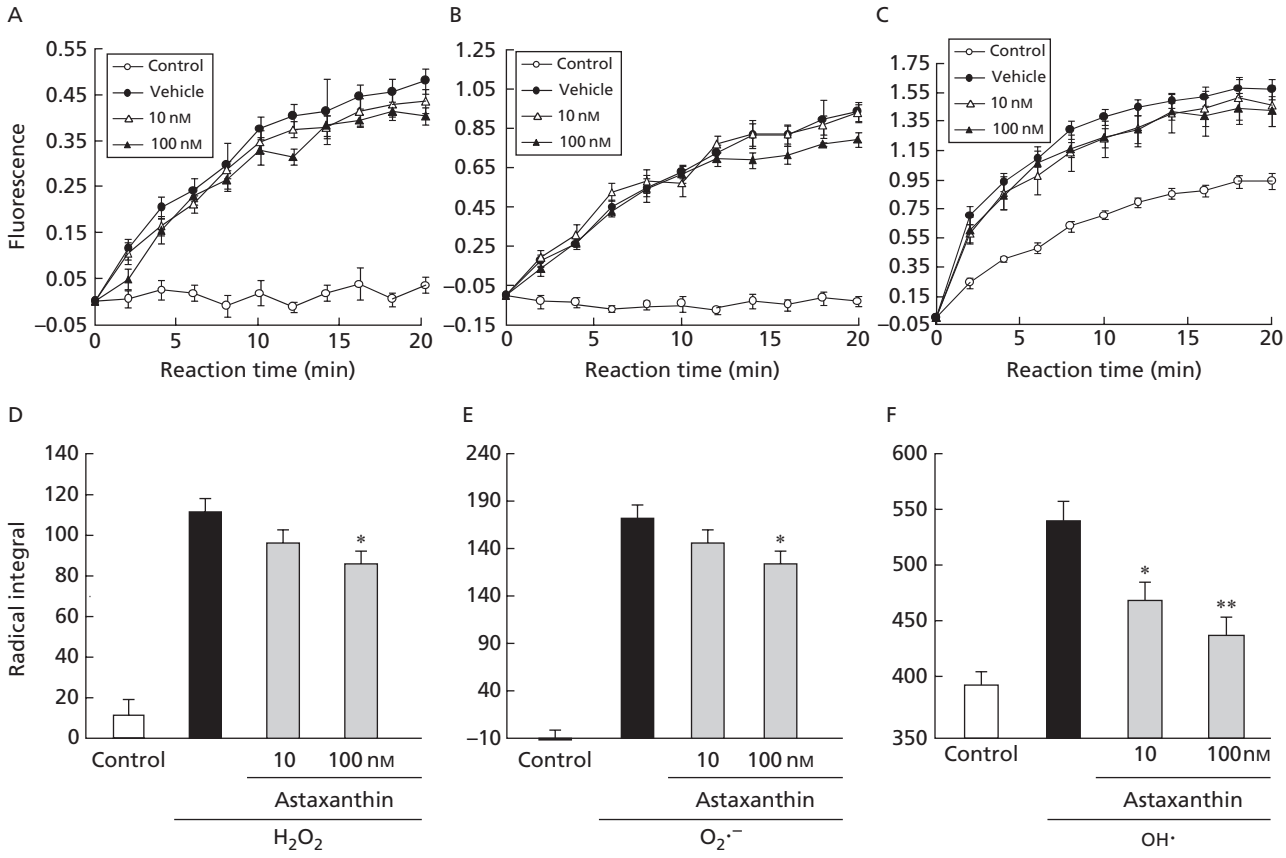

Figure 4 Astaxanthin scavenged various radical species (H_2O_2, $O_2\cdot^-$ and HO·) in RGC-5. (A–C) Time-kinetics and concentration–response relationships for antioxidant activity of astaxanthin. Astaxanthin was added to RGC-5 cultures for 1 h, then CM-H_2DCFDA (10 μM) was added for 20 min. ROS production was stimulated with H_2O_2 at 100 μM, or with KO_2 at 1 mM, or with H_2O_2 at 1 mM plus ferrous perchlorate (II) at 100 μM. Fluorescence was measured for various time periods. A. H_2O_2-induced oxidation of DCFH in RGC-5. B. $O_2\cdot^-$-induced oxidation of DCFH in RGC-5. C. HO·-induced oxidation of DCFH in RGC-5. D–F. Integral of ROS production from time-kinetic curves. Radical integral was calculated from A–C, as described in 'Methods'. Radical species were (D) H_2O_2, (E) $O_2\cdot^-$, and (F) HO·. Each column represents the mean ± s.e.m., n = 6–12. $^*P < 0.05$, $^{**}P < 0.01$ vs vehicle-treatment alone.

H_2O_2-induced cell damage was stronger than that of trolox (Figure 1D), which is a powerful free-radical scavenger, mainly of peroxynitrite ($ONOO^-$), H_2O_2, $O_2\cdot^-$, and HO· (Gupta & Sharma 2006). Astaxanthin protected cells against the cell damage induced by singlet oxygen (Schroeder & Johnson 1995), and singlet oxygen generated superoxide, hydrogen peroxide, and peroxyl radicals within the cell (Anderson et al 1974). Taken together, all this suggested that the neuroprotective effect of astaxanthin against serum deprivation-induced cell damage may have been due to a reduction in the ROS production induced by serum deprivation.

Astaxanthin protected retinal ganglion cells (RGC-5) against H_2O_2-induced and serum deprivation-induced cell death. The concentrations at which it exerted these neuroprotective effects were consistent with those which had exerted protective effects against ROS-induced intracellular oxidation (Figures 1–4). Here, we found evidence of in-vivo effects of astaxanthin against the retinal damage induced by intravitreal injection of NMDA in mice. We detected the effects of astaxanthin against the accumulation of 4-hydroxy-2-nonenal (4-HNE)-modified protein and 8-hydroxy-deoxyguanosine (8-OHdG) expression at 12 h after NMDA injection, and orally administered astaxanthin partly prevented the in-vivo retinal damage induced by NMDA in mice. The effect of astaxanthin may be attributable to attenuations of lipid peroxidation (4-HNE) and oxidative DNA damage (8-OHdG). 4-HNE, a marker of lipid peroxidation, is useful for following the progress of lipid peroxidation at the cellular level after NMDA injury. 8-OHdG is an oxidative form of the guanine nucleotide found in DNA, and so DNA that has suffered oxidative damage due to NMDA expresses 8-OHdG. Our results, therefore, indicated that astaxanthin inhibited neuronal damage in-vitro and in-vivo, and that these effects may have been partly mediated via a suppression of oxidative stress.

In this study, we administered free astaxanthin to mice. The concentrations of free astaxanthin in the plasma and liver after single-dose oral gavage with free astaxanthin have been measured by others (Showalter et al 2004). After administration of free astaxanthin (500 mg kg^{-1}, p.o.) in an emulsion vehicle to mice, the concentrations in plasma and liver tissue

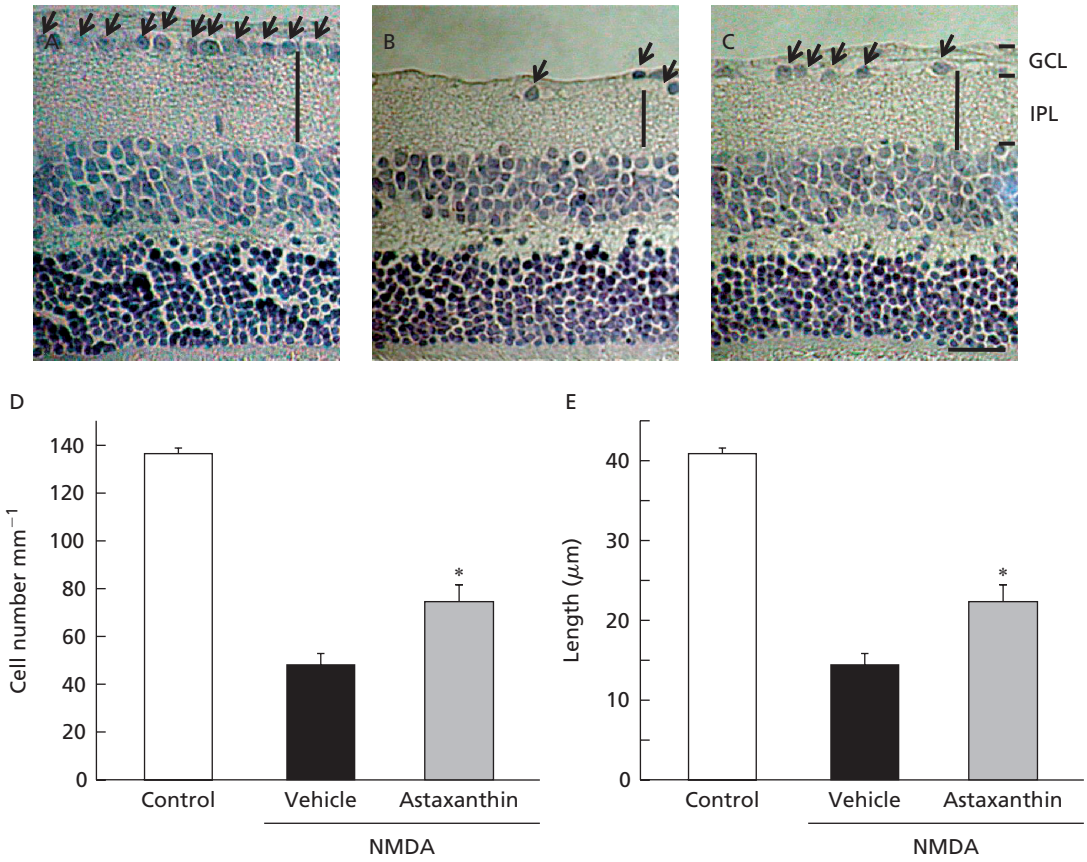

Figure 5 Effects of astaxanthin on the retinal damage observed at seven days after *N*-methyl-D-aspartate (NMDA) administration in mice. Representative photographs (haematoxylin and eosin staining of retinal sections; thickness, 5 μm) showing (A) non-treated normal retina, (B) NMDA-treated, vehicle-treated retina (control) and (C) NMDA-treated, astaxanthin-treated retina. GCL: ganglion cell layer, IPL: inner plexiform layer. Scale bar = 25 μm. Retinal damage was evaluated (D) by counting cell numbers (as indicated by arrows) in GCL and (E) by measuring the thickness of IPL (as indicated by length of vertical bar in A, B, C) in mice at seven days after intravitreal injection of either NMDA or vehicle (control). Astaxanthin was orally administered four times in all (at 6 h before, and at 0, 6 and 24 h after the NMDA injection). Each column represents the mean ± s.e.m., n = 9–11. *$P < 0.05$ vs NMDA plus vehicle treatment alone.

were 400 nM and 1.7 μM, respectively (Kurihara et al 2002; Showalter et al 2004). In this study, astaxanthin at 100 mg kg^{-1} was orally administered four times (total 400 mg kg^{-1}) within a period of 30 h (from 6 h before to 24 h after the NMDA injection) in mice. Accordingly, the maximal in-vivo concentration of astaxanthin in this study could be estimated to be at least 100 nM. In fact, astaxanthin at 100 nM or less reduced the intracellular oxidation induced by ROS (Figure 5) and in-vitro retinal ganglion cell damage (Figures 2–4).

To elucidate whether astaxanthin might protect against neuronal death in-vivo, we examined its effect on NMDA-induced retinal damage in mice. The NMDA receptor is one of the excitatory glutamate receptors whose activation leads to neuronal death, an event believed to play a role in many neurological and neurodegenerative diseases, such as cerebral ischaemia (Van der Borght et al 2005). A potential role for such excitotoxicity is also suspected in retinal diseases, such as diabetic retinopathy and glaucoma (Kalloniatis 1995). In our study, oral administration of astaxanthin (four times, each at 100 mg kg^{-1}) significantly suppressed the expression and distribution of HNE-modified protein and 8-OHdG at 12 h after NMDA injection, and protected against retinal damage at seven days after NMDA injection. Collectively, these findings suggested that orally administered astaxanthin could have neuroprotective effects against retinal damage in mice.

Conclusions

The in-vitro evidence suggested that astaxanthin exerted neuroprotective effects in RGC-5 culture, partly by reducing oxidative stress-induced ROS production. We also found that astaxanthin exerted neuroprotective effects in-vivo (against NMDA-induced retinal damage in mice), at least in part by suppressing lipid peroxidation and DNA damage. These findings suggested that astaxanthin has the potential to be an effective therapeutic drug against retinal diseases.

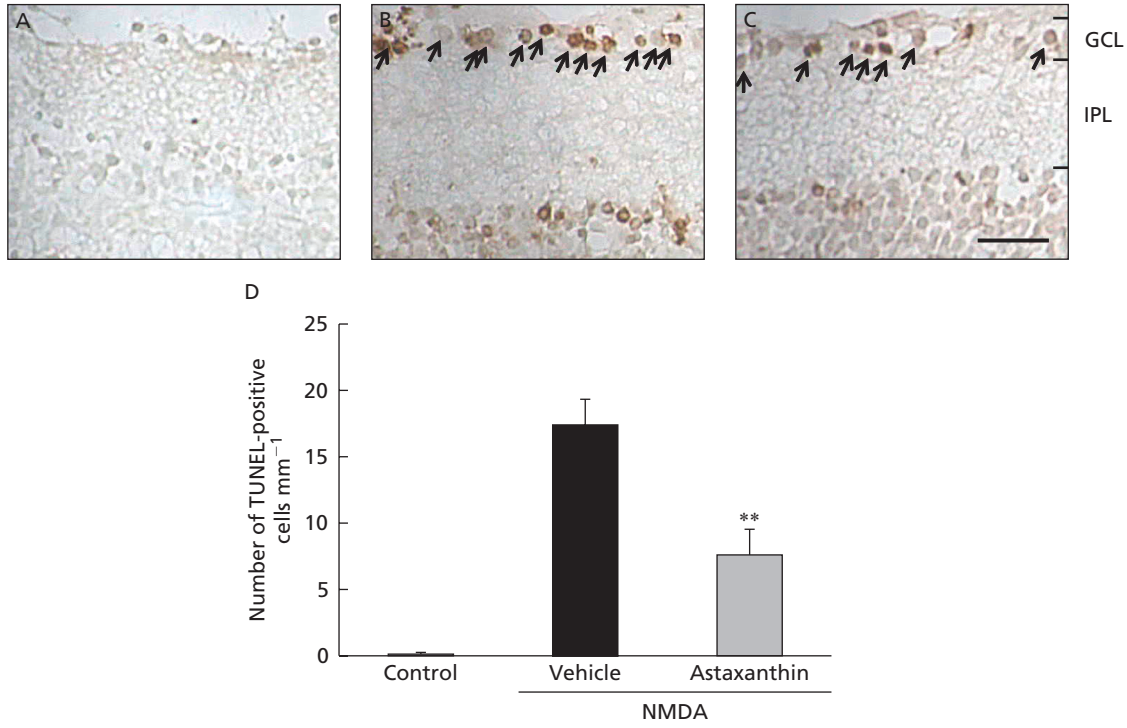

Figure 6 Astaxanthin suppressed apoptosis (TUNEL-positive cells) at 24 h after intravitreal injection of NMDA in mice. A. Non-treated normal retina. B. NMDA-treated retina (control). C. Retina treated with NMDA plus astaxanthin 100 mg kg^{-1}. Scale bar = 25 μm. D. Number of TUNEL-positive cells in ganglion cell layer (GCL). TUNEL-positive cells were localized to GCL and inner plexiform layer (IPL) in NMDA-treated retina. Arrows in B and C indicate TUNEL-positive cells. Each column represents the mean ± s.e.m., n = 8–10. $^{**}P < 0.01$ vs NMDA plus vehicle treatment alone.

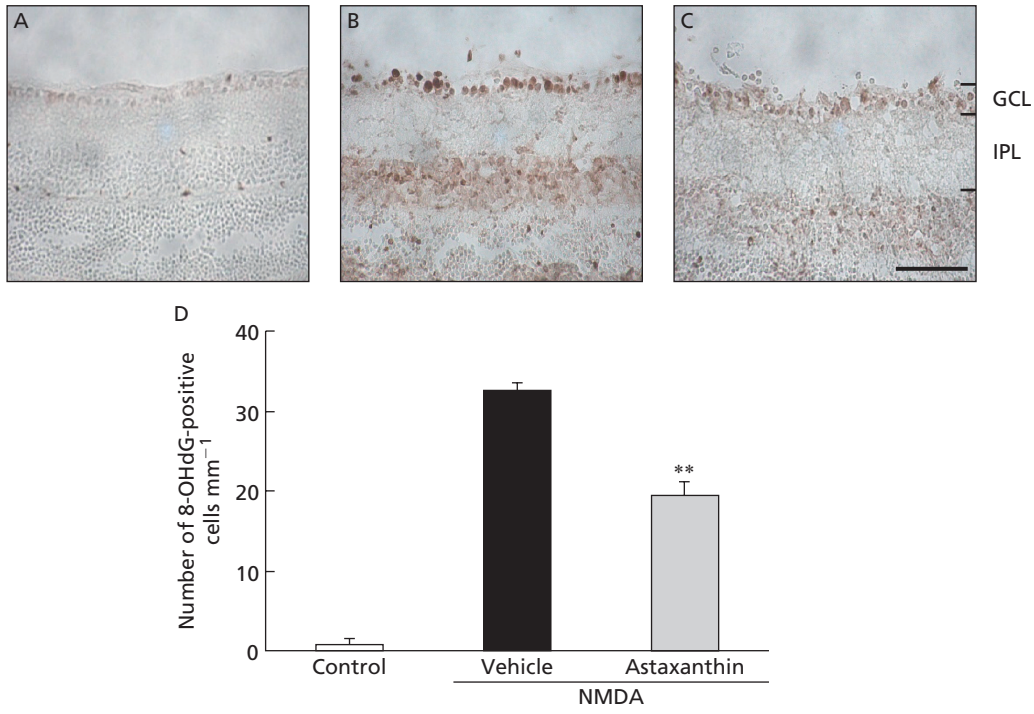

Figure 7 Effects of astaxanthin on NMDA-induced DNA damage (8-OHdG) and lipid peroxidation (4-HNE) at 12 h following intravitreal injection of NMDA in mice. Immunohistochemistry for 8-OHdG protein expression in the (A) non-treated normal retina, (B) NMDA-treated retina (control), and (C) retina treated with NMDA plus astaxanthin 100 mg kg^{-1}. (D) Number of 8-OHdG positive cells in retina. Immunohistochemistry for 4-HNE protein expression in the (E) non-treated normal retina, (F) NMDA-treated retina (control) and (G) retina treated with NMDA plus astaxanthin 100 mg kg^{-1}. (H) Quantification of 4-HNE optical density in ganglion cell layer (GCL) and inner plexiform layer (IPL). Each column represents the mean ± s.e.m., n = 5–12. $^{*}P < 0.05$, $^{**}P < 0.01$ vs NMDA plus vehicle treatment alone. Scale bar = 25 μm.

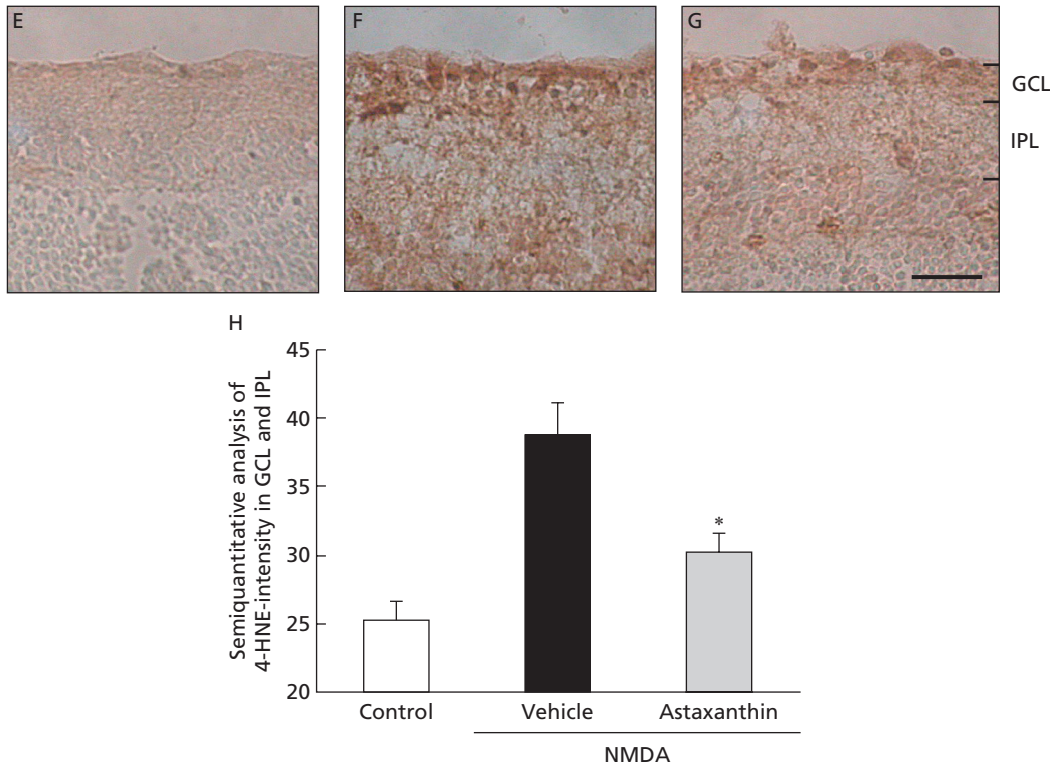

Figure 7 *(Continued)*

References

Anderson, S. M., Krinsky, N. I., Stone, M. J., Clagett, D. C. (1974) Effect of singlet oxygen quenchers on oxidative damage to liposomes initiated by photosensitization or by radiofrequency discharge. *Photochem. Photobiol.* **20**: 65–69

Aoi, W., Naito, Y., Sakuma, K., Kuchide, M., Tokuda, H., Maoka, T., Toyokuni, S., Oka, S., Yasuhara, M., Yoshikawa, T. (2003) Astaxanthin limits exercise-induced skeletal and cardiac muscle damage in mice. *Antioxid. Redox. Signal.* **5**: 139–144

Bocker-Meffert, S., Rosenstiel, P., Roho, C., Warneke, N., Held-Feindt, J., Sievers, J., Lucius, R. (2002) Erythropoietin and VEGF promote neural outgrowth from retinal explants in postnatal rats. *Invest. Ophthalmol. Vis. Sci*. **43**: 2021–2026

Bonne, C., Muller, A., Villain, M. (1998) Free radicals in retinal ischemia. *Gen. Pharmacol.* **30**: 275–280

Chew, B. P., Park, J. S., Wong, M. W., Wong, T. S. (1999a) A comparison of the anticancer activities of dietary beta-carotene, canthaxanthin and astaxanthin in mice in vivo. *Anticancer Res.* **19**: 1849–1853

Chew, B. P., Wong, M. W., Park, J. S., Wong, T. S. (1999b) Dietary beta-carotene and astaxanthin but not canthaxanthin stimulate splenocyte function in mice. *Anticancer Res.* **19**: 5223–5227

Clarke, J. B., Eliopoulos, E. E., Findlay, J. B., Zagalsky, P. F. (1990) Alternative ligands as probes for the carotenoid-binding site of lobster carapace crustacyanin. *Biochem. J.* **265**: 919–921

Dreyer, E. B. (1998) A proposed role for excitotoxicity in glaucoma. *J. Glaucoma* **7**: 62–67

Gupta, S., Sharma, S. S. (2006) Neuroprotective effects of trolox in global cerebral ischemia in gerbils. *Biol. Pharm. Bull.* **29**: 957–961

Iwamoto, T., Hosoda, K., Hirano, R., Kurata, H., Matsumoto, A., Miki, W., Kamiyama, M., Itakura, H., Yamamoto, S., Kondo, K. (2000) Inhibition of low-density lipoprotein oxidation by astaxanthin. *J. Atheroscler. Thromb.* **7**: 216–222

Jyonouchi, H., Sun, S., Iijima, K., Gross, M. D. (2000) Antitumor activity of astaxanthin and its mode of action. *Nutr. Cancer* **36**: 59–65

Kalloniatis, M. (1995) Amino acids in neurotransmission and disease. *J. Am. Optom. Assoc.* **66**: 750–757

Kang, J. O., Kim, S. J., Kim, H. (2001) Effect of astaxanthin on the hepatotoxicity, lipid peroxidation and antioxidative enzymes in the liver of CCl4-treated rats. *Methods Find Exp. Clin. Pharmacol.* **23**: 79–84

Kim, Y. H., Takahashi, M., Noguchi, N., Suzuki, E., Suzuki, K., Taniguchi, N., Niki, E. (2000) Inhibition of c-Jun expression induces antioxidant enzymes under serum deprivation. *Arch. Biochem. Biophys.* **374**: 339–346

Kobayashi, M. (2000) In vivo antioxidant role of astaxanthin under oxidative stress in the green alga *Haematococcus pluvialis*. *Appl. Microbiol. Biotechnol.* **54**: 550–555

Kurashige, M., Okimasu, E., Inoue, M., Utsumi, K. (1990) Inhibition of oxidative injury of biological membranes by astaxanthin. *Physiol. Chem. Phys. Med. NMR* **22**: 27–38

Kurihara, H., Koda, H., Asami, S., Kiso, Y., Tanaka, T. (2002) Contribution of the antioxidative property of astaxanthin to its protective effect on the promotion of cancer metastasis in mice treated with restraint stress. *Life Sci.* **70**: 2509–2520

McKinnon, S. J. (1997) Glaucoma, apoptosis, and neuroprotection. *Curr. Opin. Ophthalmol.* **8**: 28–37

Neufeld, A. H. (1999) Nitric oxide: a potential mediator of retinal ganglion cell damage in glaucoma. *Surv. Ophthalmol.* **43** (Suppl. 1): S129–S135

O'Connor, I., O'Brien, N. (1998) Modulation of UVA light-induced oxidative stress by beta-carotene, lutein and astaxanthin in cultured fibroblasts. *J. Dermatol. Sci.* **16**: 226–230

Ohgami, K., Shiratori, K., Kotake, S., Nishida, T., Mizuki, N., Yazawa, K., Ohno, S. (2003) Effects of astaxanthin on lipopolysaccharide-induced inflammation in vitro and in vivo. *Invest. Ophthalmol. Vis. Sci.* **44**: 2694–2701

Okai, Y., Higashi-Okai, K. (1996) Possible immunomodulating activities of carotenoids in in vitro cell culture experiments. *Int. J. Immunopharmacol*. **18**: 753–758

Parisi, V., Tedeschi, M., Gallinaro, G., Varano, M., Saviano, S., Piermarocchi, S. (2008) Carotenoids and antioxidants in age-related maculopathy Italian study: multifocal electroretinogram modifications after 1 year. *Ophthalmology* **115**: 324–333

Schlieve, C. R., Lieven, C. J., Levin, L. A. (2006) Biochemical activity of reactive oxygen species scavengers do not predict retinal ganglion cell survival. *Invest. Ophthalmol. Vis. Sci*. **47**: 3878–3886

Schroeder, W. A., Johnson, E. A. (1995) Singlet oxygen and peroxyl radicals regulate carotenoid biosynthesis in *Phaffia rhodozyma*. *J. Biol. Chem.* **270**: 18374–18379

Shimazawa, M., Yamashima, T., Agarwal, N., Hara, H. (2005) Neuroprotective effects of minocycline against in vitro and in vivo retinal ganglion cell damage. *Brain Res*. **1053**: 185–194

Showalter, L. A., Weinman, S. A., Osterlie, M., Lockwood, S. F. (2004) Plasma appearance and tissue accumulation of non-esterified, free astaxanthin in C57BL/6 mice after oral dosing of a disodium disuccinate diester of astaxanthin (Heptax). *Comp. Biochem. Physiol. C Toxicol. Pharmacol.* **137**: 227–236

Siliprandi, R., Canella, R., Carmignoto, G., Schiavo, N., Zanellato, A., Zanoni, R., Vantini, G. (1992) N-methyl-D-aspartate-induced neurotoxicity in the adult rat retina. *Vis. Neurosci.* **8**: 567–573

Uchiyama, K., Naito, Y., Hasegawa, G., Nakamura, N., Takahashi, J., Yoshikawa, T. (2002) Astaxanthin protects beta-cells against glucose toxicity in diabetic db/db mice. *Redox. Rep.* **7**: 290–293

Van der Borght, K., Mulder, J., Keijser, J. N., Eggen, B. J., Luiten, P. G., Van der Zee, E. A. (2005) Input from the medial septum regulates adult hippocampal neurogenesis. *Brain Res. Bull.* **67**: 117–125

Yoneda, S., Tanihara, H., Kido, N., Honda, Y., Goto, W., Hara, H., Miyawaki, N. (2001) Interleukin-1beta mediates ischemic injury in the rat retina. *Exp. Eye. Res.* **73**: 661–667